# Measuring Radiation Yield in EB Polymerizations via Raman Spectroscopy

*Nicole Kloepfer,[1] Sage M. Schissel,[2] Julie L. P. Jessop[1]*
*[1]University of Iowa, Iowa City, IA 52242*
*[2]ebeam Technologies, Davenport, IA 52806*

## Abstract

For photopolymerization, many methods exist to determine kinetic parameters, such as quantum yield of photoinitiators and rate of photoinitiation. However, due to the harsh conditions of the electron beam (EB), relatively few studies have examined the kinetics of EB polymerization. Here, a new method for determining rate of initiation and radiation yield (the number of radicals per 100 eV delivered) using Raman spectroscopy is presented, which will enable more detailed kinetic studies of EB polymerization.

## Background

The major difference in ultraviolet (UV) and electron-beam (EB) polymerization lies within the initiation mechanism.[1] In a generalized mechanistic description of UV initiation, a photoinitiator molecule (*I*) absorbs energy, which causes the photoinitiator to decompose into two primary radical species ($R^{\bullet}$). One or both radical species can then react with a monomer molecule (*M*) to form an activated monomer ($M^{\bullet}$) (Scheme 1).

$$I \xrightarrow{h\nu} 2R^{\bullet}$$
$$R^{\bullet} + M \rightarrow M^{\bullet}$$

**Scheme 1.** The UV-initiation mechanism. Adapted from Reference 1.

The resulting rate of initiation ($R_i$) is described by the following equation:

$$R_i = 2\phi I_a \tag{1}$$

where $I_a$ is the intensity of absorbed light (moles of light quanta per liter·second) and $\phi$ is the quantum yield (number of propagating chains initiated per light photon absorbed).[1]

During EB initiation, ionizing radiation provides sufficient energy to generate primary radicals directly on the monomer molecules:

$$M \rightarrow 2R^{\bullet} \tag{2}$$

The resulting rate of radical formation ($R_R$) is described by the following equation:

$$R_R = G_R \rho \frac{dD}{dt} \tag{3}$$

where $G_R$ is the radiation yield (number of radicals created by 100 eV of energy absorbed by the system), $\rho$ is the density of the system (g/mL), and $\frac{dD}{dt}$ is the dose rate (kGy/s).[2]

Unlike photoinitiated systems, the primary radicals generated by the EB often undergo further reactions,[3] including: recombination (reaction of two primary radicals to form a small molecule), initiation (reaction of a primary radical and a monomer molecule to form a growing polymer chain), crosslinking (reaction of two primary radicals on the backbone of a growing polymer chain $P - R^{\bullet}$ to form a network connection $X$), or termination (reaction of a primary radical and a growing polymer chain to form a dead polymer $P_n$). Other primary radicals will be inherently inert or trapped by the forming network and will not undergo further reactions (Scheme 2).

| | |
|---|---|
| Recombination: | $R^{\bullet} + R^{\bullet} \rightarrow R_2$ |
| Initiation: | $R^{\bullet} + M \rightarrow RM^{\bullet}$ |
| Crosslinking: | $P - R^{\bullet} + P - R^{\bullet} \rightarrow X$ |
| Termination: | $M_n{}^{\bullet} + R^{\bullet} \rightarrow P_n$ |
| Inert/Trapped: | $R^{\bullet} \rightarrow no\ reaction$ |

**Scheme 2.** Possible reactions of primary radicals formed during EB initiation. Adapted from Reference 3.

Because the primary radicals can react in many ways, the total number of primary radicals does not completely describe the complex system. Thus, the radiation yield can be described as the sum of the initiating radical radiation yield ($G_i$, number of radicals that initiate polymerization per 100 eV of energy absorbed by the system), crosslinking radical radiation yield ($G_x$, number of radials that cause crosslinking events per 100 eV delivered to the system), terminating radical radiation yield ($G_t$, number of primary radicals that only react to terminate polymer chains per 100 eV delivered to the system), and the unreactive radical radiation yield ($G_n$, number of radicals that fail to interact with the network per 100 eV of energy delivered to the system) shown in Equation 4.

$$G_R = G_i + G_x + G_t + G_n \tag{4}$$

If all the primary radicals further react with monomer molecules to initiate polymerization (*i.e.*, $G_R = G_i$), then the rate of initiation ($R_i$) can be expressed as

$$R_i = G_i \rho \frac{dD}{dt} \tag{5}$$

The assumption $G_R = G_i$ is often made, and Equation 5 is used to describe the rate of initiation of EB polymerization.[2,3] However, during a typical EB polymerization, all the reactions portrayed in Scheme 2 take place, and Equation 5 may not be valid.

To further complicate the matter, measuring the concentration of radicals directly is very difficult. The number of radicals is often determined by adding a compound that will react with any radicals in the system and that is easily measured via spectroscopy or another analytical technique. This method for determining radical concentration will only count the reactive radicals, and the yield that is measured is the apparent radiation yield $G_R{}'$:

$$G_R' = G_i + G_x + G_t \quad (6)$$

The apparent radiation yield only accounts for the radicals that are important to polymerization and network formation.

The fraction of propagating radicals ($f_i$), crosslinking radicals ($f_x$), and terminating radicals ($f_t$) can be determined from the ratio of *G*-values:

$$f_i = \frac{G_i}{G_R'} \quad (7)$$

The sum of $f_i$, $f_x$, and $f_t$ is one, as these three *f*-values account for all the measurable radicals formed by the EB. These *f*-values provide insight into network formation and can be used to relate the apparent radiation yield to the rate of initiation as follows:

$$R_i = f_i G_R' \frac{dD}{dt} \quad (9)$$

Calculation of *G*-values for EB-initiated polymer systems has proven difficult, and after an extensive literature search, $G_R'$ of only a handful of continuous EB-initiated monomer have been found.[2,4-6] One method used to determine $G_R'$ relies on building a kinetic profile (conversion vs. time), calculating the resulting gel fraction, and determining of the number-averaged degree of polymerization ($X_n$).[4] Not only does this method require multiple experiments, it is also necessary to make numerous assumptions about network formation, rate of polymerization, and termination that may not be appropriate for all systems. As a result, it is desirable to develop a new method to determine $G_R'$ and/or $G_i$ for EB reactions that is easier to implement and can be used for any monomer.

Other methods for determining *G*-values have been developed for gamma-initiated systems, but these methods have not been implemented for EB-initiated systems.[2] Furthermore, in the gamma-initiated polymerization literature, $G_i$, $G_R$, and $G_R'$ are not carefully defined and the different *G*-values are often used interchangeably.[2] Modification to these methods will allow distinct *G*-values to be determined for EB-initiation.

Determination of the radiation yields (*i.e.*, *G*-values) and investigation of the kinetics of EB polymerization will help develop formulation chemistry/processing conditions/polymer properties relationships that are lacking in EB-initiated systems. Furthermore, with careful experimental design, both $G_R'$ and $G_i$ can be determined and compared to provide insight into the number and types of radicals that are formed during EB exposure.

## Experimental

### Materials

The monomer benzyl acrylate (BA, TCI America) was chosen to investigate the radiation yield during EB initiation. Experiments carried out under UV irradiation were photoinitiated by 2,2-dimethoxy-2-phenylacetophenone (DMPA, Sartomer). If an inhibitor was required for the experiment, hydroquinone (HQ, TCI America) was used. Finally, the solvent used in the

experiments was tetrahydrofuran (THF, Aldrich). THF was filtered through 0.2 μm nylon filter disks (Cole Parmer) and degassed before use, and all other materials were used as received and stored at room temperature.

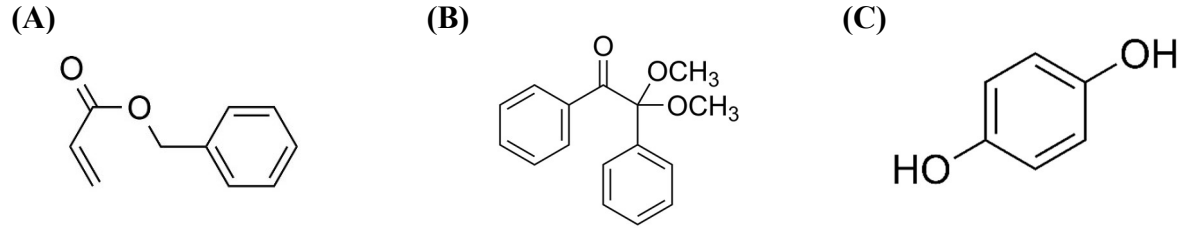


**Figure 1.** Chemical structure of A) monomer BA, B) photoinitiator DMPA, and C) inhibitor HQ.

## Methods

### *Protocol 1*

*Sample Preparation.* Formulations of neat BA and BA containing five concentrations of inhibitor HQ (0.25%, 0.5%, 1.0%, 1.5%, and 2.0% by weight) were prepared and sonicated for 30 min to ensure complete mixing. A controlled volume of each formulation was pipetted into an aluminum dish to create a 200-micron thick film. Dishes were attached to aluminum Q-panels for easier sample handling, resulting in 10 panels of neat monomer and each of the monomer/inhibitor formulations.

*Electron-Beam Exposure.* EB exposure was performed on a EBLab unit (Comet Technologies, Inc.). The voltage was set at 200 kV, and nitrogen flow was used to reduce the oxygen concentration to less than 200 ppm to minimize the effects of oxygen inhibition. Each panel was exposed to a unique dose of radiation, while the dose rate was held constant by controlling the line speed. Dose and line speed combinations are shown in Table 1.

**Table 1.** Dose and line speed combinations used to create the kinetic profiles for the inhibition experiments.

| **Dose (kGy)** | 200 | 100 | 67 | 50 | 40 | 33 | 29 | 25 | 22 | 20 |
|---|---|---|---|---|---|---|---|---|---|---|
| **Line speed (m/min)** | 3 | 6 | 9 | 12 | 15 | 18 | 21 | 24 | 27 | 30 |

*Raman Analysis.* After polymerization, the EB samples were transferred to quartz capillary tubes, and Raman spectroscopy was used to determine the conversion. To eliminate error from instrumental variations, a reference peak was used. Previous work has established the reaction peak at 1636 $cm^{-1}$ (indicative of the -C=C- bond in the acrylate moiety) and the reference peak at 1613 $cm^{-1}$ (indicative of the -C=C- bonds in the phenyl ring).[7] Conversion was calculated using the following equation:

$$\alpha = \left(1 - \frac{I_{rxn}(P)/I_{ref}(P)}{I_{rxn}(M)/I_{ref}(M)}\right) * 100 \quad (8)$$

where $I_{rxn}(P)$ and $I_{ref}(P)$ are the peak intensities of the reaction and reference peak of the polymer, respectively; $I_{rxn}(M)$ and $I_{ref}(M)$ are the peak intensities of the reaction and reference peak of the monomer.[8]

Raman spectra of the samples were collected using a holographic probe head (Mark II, Kaiser Optical Systems Inc.) connected to a modular research Raman spectrograph (HoloLab 5000R, Kaiser Optical Systems, Inc.) via a 100 μm collection fiber. A single-mode excitation fiber carried an incident beam of 785 nm near-infrared laser to the quartz capillary tube. Laser power at the sample was approximately 180 mW. Spectra were collected with an exposure time of 250 ms and 5 accumulations. Ten monomer and sample spectra were collected and averaged to provide accurate values for Equation 8, and conversions were reported.

***Protocol 2***

*Real-Time Raman Spectroscopy.* Formulations of BA containing five different concentrations of initiator DMPA (0.1%, 0.2%, 0.3%, 0.4%, and 0.5% by weight) were created and pipetted into capillary tubes. Real-time Raman spectroscopy was used to monitor conversion during illumination with a mercury arc lap fitted with a 250-450 nm filter (Omnicure Ultraviolet/Visible Spot Cure system, EXFO Photonic Solutions Inc.) for 30 seconds at an effective irradiance of 1.74 W/cm$^2$ as measured with a radiometer (R2000, Omnicure, wavelength range 250 nm – 1 μm). Spectra were acquired using the same setup as described in Protocol 1. The spectra were collected with 0.5 second exposure time and 1 accumulation during illumination. Ten monomer spectra were collected before illumination and averaged to provide accurate values for Equation 8. After illumination, conversion was calculated using Equation 8 as described in Protocol 1. The conversion data was used to calculate the rate of polymerization ($R_p$), which is equal to the rate of disappearance of monomer ($\frac{d[M]}{dt}$). The instantaneous concentration of monomer ($[M]$) was determined using the following equation:

$$[M] = [M]_0(1 - \alpha) \tag{9}$$

where $[M]_0$ is the initial monomer concertation. A linear best fit line was drawn through the data points, and the negative slope of the best fit line was equal to $R_p$.

*Gel Permeation Chromatography (GPC).* The same formulations of BA and initiator used for real-time Raman analysis were used for GPC analysis. Glass slides were coated with two layers of Rain-X ®, glass cover slips were placed on each side of one glass slide to act as a spacer, a second glass slide was placed on top of the cover slips such that the Rain-X coated sides were both facing inward, and the mold was clamped together with binder clips on each end. Each mold was injected with one of the five formulations of BA containing DMPA. The samples were illuminated with a UV belt lamp system (Fusion UV Systems, Inc.) equipped with a mercury arc lamp with an effective irradiance of 1.7 W/cm$^2$. After illumination, the films were removed from the molds and transferred to vials that were filled with tetrahydrofuran (THF) and allowed to dissolve for 48 hours. Finally, the samples were filtered through number one filter paper (Whitman).

The filtrate was injected through a 20 μL loop, and THF pushed the sample through the GPC system at a flow rate of 1.0 mL/min. The sample was fractionated by a PL-gel 5μm mixed-D column (Agilent Inc.) before multi-angle light scattering analysis (DAWN HELEOS-II, Wayatt Technology) and refractive index measurements (Optilab T-Rex, Wayatt Technology) were performed. Data analysis gave the number-averaged molecular weight $\bar{M}_n$, which was used to determine $\bar{X}_n$ via the following equation:

$$\bar{M}_n = M_r \bar{X}_n \tag{10}$$

where $M_r$ is the molecular weight of the repeat unit.[1]

*Raman Spectroscopy of EB samples.* Neat BA was exposed to the EB, and the conversion of each sample was analyzed using Raman spectroscopy as described in Protocol 1.

## Results and Discussion

### Protocol 1

Protocol 1 was adapted from a method to determine what the authors referred to as $G_R$ of monomers initiated with gamma radiation.[2] The protocol measures what has been defined in this paper as $G_R{}'$. In Protocol 1, inhibitor HQ was added to the formulations to react with primary radicals, which delayed conversion until all the inhibitor was exhausted. Because each inhibitor molecule reacts with one radical, the change in concentration of inhibitor was equivalent to the apparent rate of radical formation $R_R'$. The apparent radiation yield $G_R{}'$ was then calculated according to the following equation.

$$R_R' = G_R{}'\rho\frac{dD}{dt} \tag{11}$$

#### *Inhibition Time*

A kinetic profile of conversion vs. time was built for neat BA and BA containing each of the five concentrations of inhibitor. The inhibition period was determined for each formulation as the intersection of two best fit lines; the first through the points with less than 5% conversion, and the second through the remaining points at higher conversion. A representative kinetic profile of neat BA is shown in Figure 2. The goodness of fit, reported as the $R^2$ values, was above 0.9855 for all the greater than 5% conversion trendlines. The trendlines for the less than 5% conversion data had significantly lower $R^2$ values that ranged between 0.058 and 0.9801. The low $R^2$ values can be attributed to the large amount of Raman error at low conversions. Because the conversion is not yet increasing, the large, random variation in Raman measurements drastically reduces the goodness of fit.

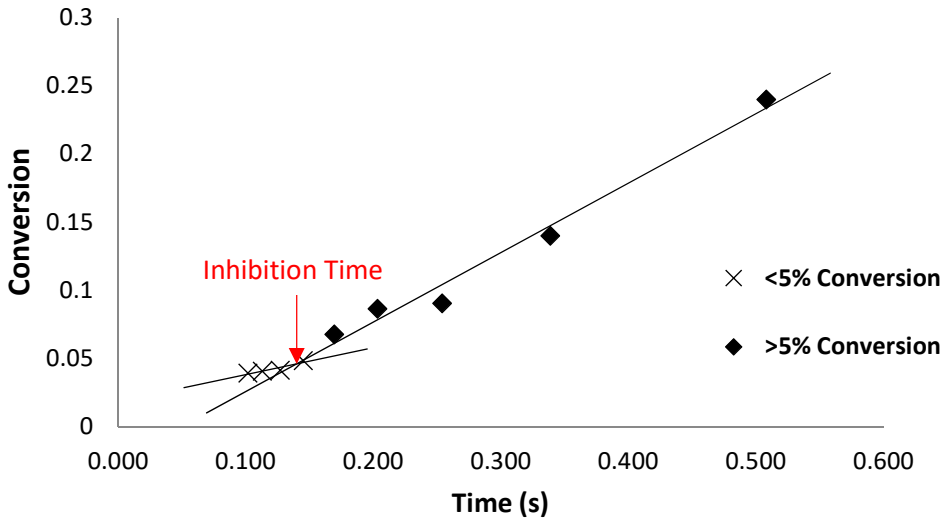


**Figure 2.** The kinetic profile of neat BA used to calculate the inhibition period.

Because dissolved oxygen inhibits conversion, even neat BA exhibited some inhibition period. To determine the inhibition in each formulation caused by HQ and not dissolved oxygen, the inhibition period of neat BA was subtracted from the inhibition period for each formulation; the result is reported as inhibition time (Table 2).

**Table 2.** The inhibition times resulting from the addition of HQ.

| **Concentration HQ (wt. %)** | **0.25%** | **0.5%** | **1.0%** | **1.5%** | **2.0%** |
|---|---|---|---|---|---|
| **Inhibition time (s)** | 0.003 | 0.024 | 0.074 | 0.046 | 0.167 |

***Rate of Radical Formation***

Inhibitor concentration in mol/L was plotted as a function of the resulting inhibition times, and a best fit line was drawn through the data points (Figure 3). The slope of the best fit line was 0.9664 mol/L·s, which is equal to the change in inhibitor concentration with respect to time. Because each inhibitor molecule reacts with one radicals, the slope is also equal to the apparent rate of radical formation, $R_R'$.

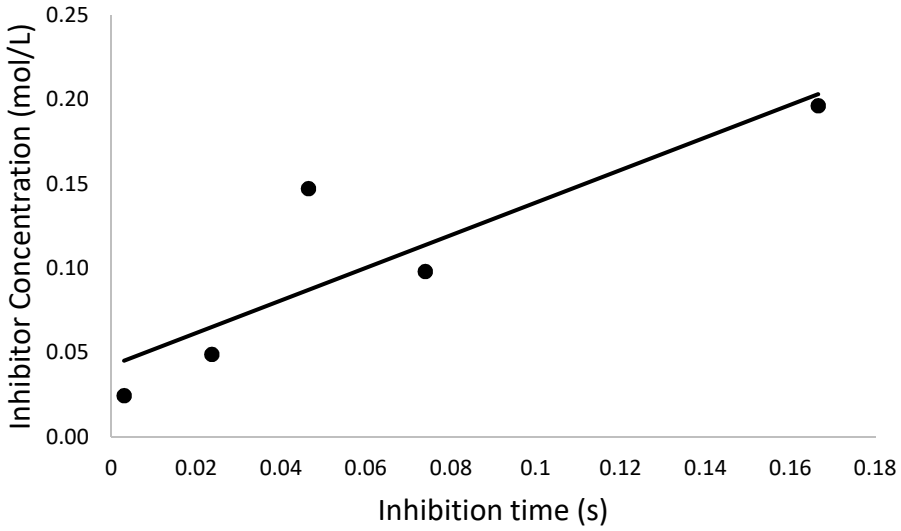


**Figure 3.** Inhibitor concentration vs. inhibition time. The slope of the resulting trend line is the change in inhibitor concentration with respect to time, which is equal to the apparent rate of radical formation. The goodness of fit, reported as $R^2$ values, was above 0.7449 for all three trials.

### *Apparent Radiation Yield $G_R$'*

Equation 11 was used to calculate $G_R{}'$. Because numerous unit conversions are necessary, a sample calculation is provided and explained below.

$$G_R' = \frac{R_R'}{\rho \frac{dD}{dt}} = \frac{0.9664\ mol\ L^{-1}\ s^{-1}}{1.06\ g\ mL^{-1} \times 197 kGy\ s^{-1}} \times \frac{kGy}{Jg^{-1}} \times \frac{J}{6.242 \times 10^{18} eV} \times \frac{L}{1000\ mL} \times \frac{6.022 \times 10^{23}}{mol} \times 100 eV = \mathbf{45}$$

First, the dose was converted from $kGy$ to the SI units $\frac{J}{g}$. A second conversion was used to transform the energy from $J$ to $eV$. The volume units in the density term were converted from $mL$ to $L$. Next, Avogadro's Number was used to convert from a molar basis to a radical basis. Finally, the answer was multiplied by 100 eV so that the reported value would be consistent with the definition of radiation yield. Three trials were conducted, and the resulting $G_R'$ values are reported in Table 3.

**Table 3.** The apparent radiation yield values resulting from three trials of Protocol 1.

| | **Trial 1** | **Trial 2** | **Trial 3** |
|---|---|---|---|
| **Apparent Radiation Yield, $G_R{}'$** | 45 | 30 | 99 |

The average $G_R'$ resulting from the three trials is 60±40. The standard deviation in the $G_R'$ value is very large. Some error can be attributed to the noise in the Raman measurements, which is typically ±5%. If each data point in the kinetic profile has an error of ±5%, that error propagates and intensifies when the profile is used to determine the inhibition time. Raman measurements are not the only source of error. The initiation mechanism of the EB is not well

understood at this time and often regarded as a series of random reactions and chain reactions. Because the ionizing radiation provided by the EB can react with the formulation in so many ways, radical formation might not take place at the same rate in every sample. To minimize the error, other methods for following the disappearance of inhibitor, such as UV-Vis spectroscopy, will be explored in future experiments.

**Protocol 2**

Protocol 2 was adapted from a method to determine quantum yield in initiators during photopolymerizations.[1] In Protocol 2, the propagating radical radiation yield, $G_i$, was calculated from Equation 5. To determine $R_i$ necessary for this calculation, a ratio of the kinetic constant of propagation $k_p$ and the kinetic constant of termination $k_t$, as well as the rate of EB propagation $R_P$, are needed.

***Kinetic Constants in Photopolymerization***

Because the propagation and termination steps of EB and UV polymerizations are thought to be the same, the kinetic constants of propagation and termination are also considered equivalent for both initiation mechanisms. The ratio of the kinetic constants can be related to $R_p$, $\bar{X}_n$, and a constant for chain transfer to the monomer ($C_M$) as follows:

$$\frac{1}{\bar{X}_n} = \frac{k_t R_p}{2{k_p}^2[M]^2} + C_M \tag{12}$$

$R_p$ was calculated from real-time Raman data, and $\bar{X}_n$ was calculated from GPC data. A graph of $\frac{1}{\bar{X}_n}$ vs. $\frac{R_p}{[M]^2}$ is shown in Figure 4. A linear best fit line was drawn though the data points, resulting in a slope of 0.1578 mol·s/L, which is equal to $\frac{k_t}{2{k_p}^2}$. Thus, the ratio of the kinetic constants $\frac{k_t}{{k_p}^2}$ needed to calculate the rate of EB polymerization was determined to be 0.3156 mol·s/L.

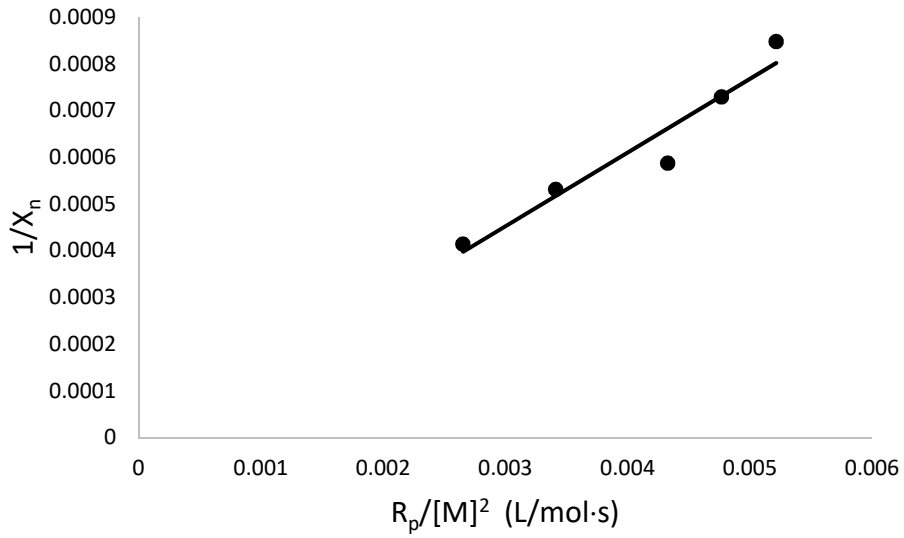


**Figure 4.** A plot of Equation 12 for the photopolymerization of neat BA. The slope of the linear best fit line was used to determine the ratio of the kinetic constants of propagation and termination $\left(\frac{k_t}{{k_p}^2}\right)$. The goodness of fit, reported as the $R^2$ value, was equal to 0.93.

***Rate of EB Polymerization***

Because real-time Raman measurements are not possible during EB polymerization, the kinetic profile could not be constructed in the same manner as described for the photopolymerization experiments. Instead, the conversion was determined for individual samples that received increasing doses of radiation. The kinetic profile was then pieced together from the conversion measurements of successive experiments. Once the kinetic profile was constructed, the method to determine $R_p$ was followed from the photopolymerization experiments. The instantaneous concentration of monomer was determined using Equation 9, and $R_p$ was calculated as the negative slope of the best fit line. The disappearance of monomer as a function of time for the EB polymerization reaction is shown in Figure 5. A linear best fit line was drawn through the data points with greater than 5% conversion, and the resulting slope was -3.3 mol/L·s. Thus, $R_p$ for the EB polymerization of neat BA was determined to be 3.3 mol/L·s.

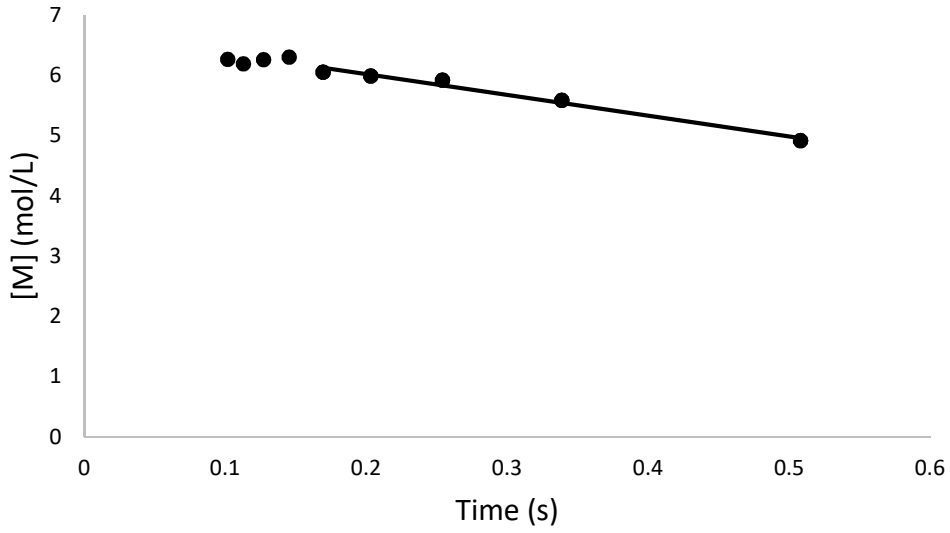


**Figure 5.** The disappearance of neat BA during EB polymerization. The slope of the best fit line through the data points with greater than 5% conversion was equal to the negative rate of EB polymerization. The goodness of fit, reported as the $R^2$ value, was greater than 0.9809 for all three trials.

***Propagating Radical Radiation Yield $G_i$***

Assuming radical formation reaches steady state, Equation 14 can be used to determine the rate of EB initiation as follows:[1]

$$R_i = \frac{k_t}{{k_p}^2}\frac{{R_p}^2}{[M]^2} \tag{14}$$

Equation 14 was used to calculate $R_i$, and from that, $G_i$ was calculated using Equation 5. Three trials were conducted, and the resulting $G_i$ values are reported in Table 4.

**Table 4.** The propagating radical radiation yields resulting from three trials of Protocol 2.

| | **Trial 1** | **Trial 2** | **Trial 3** |
|---|---|---|---|
| **Propagating Radical Radiation Yield, $G_i$** | 3.7 | 3.2 | 3.6 |

The average $G_i$ value resulting from the three trials was 3.5±0.3, which is considerably lower than the calculated ${G_R}'$. Using Equation 7, the fraction of propagating ($f_i$) radicals is 0.06. EB reactions often result in highly crosslinked polymer, so it may not be surprising only a small fraction of primary radicals react to form propagating radicals. However, Equation 5 is used to calculate $G_i$ and is only valid if all the primary radicals react with monomer to become propagating radicals, which clearly is not the case. In future work, other models will be explored to more accurately determine $G_i$ for systems with additional reactions of primary radicals.

## Conclusions

Preliminary protocols have been developed to determine the apparent radiation yield $G_R{}'$ and the propagating radical radiation yield $G_i$. These protocols produced results consistent with the fact that there should be more primary radicals than propagating radicals, but each protocol has room for improvement. The error in Protocol 1 needs to be reduced, and future work should focus on lowering the Raman variation or seek alternate methods to monitor the disappearance of inhibitor, such as UV-Vis. The assumption made in Protocol 2 is an oversimplification of the EB initiation mechanism, and additional details are needed to provide more accurate results. These two methods provide a solid basis for future work and have potential to uncover some of the mysteries of EB initiation, but work is still needed to perfect the techniques.

## Acknowledgements

This material is based upon work supported by the National Science Foundation under Grant No. 1264622 and The University of Iowa Mathematical & Physical Sciences Funding Program. The authors would also like to acknowledge Kyle McCarthy and Renae Kurpius for their contributions to data collection.

## References

[1] Odian, G., *Principles of Polymerization, fourth ed*. John Wiley & Sons, Inc.: New Jersey, **2004**.

[2] Chapiro, A., *Radiation Chemistry of Polymeric Systems*. John Wiley & Sons, Inc.: New York, **1962**.

[3] Richter, K.B., *Pulsed Electron Beam Curing of Polymer Coatings*. Proquest: Michigan, **2007**.

[4] Labana, S.S., Kinetics of high-intensity electron-beam polymerization of a divinyl urethane. *J. Polym. Sci. Part A-1: Polym. Chem*. 6(12), **1986**, pp. 3283–3293.

[5] Squire, D. R., Cleaveland, J. A., Hossain, T. M. A., Oraby, W., Stahel, E. P., and Stannett, V. T., Studies in Radiation-Induced Polymerization of Vinyl Monomers at High Dose Rates. I. Styrene. *J. Appl. Polym. Sci*. Vol 16, **1972**, pp. 645-661.

[6] Allen, C. C., Oraby, W., Hossain, T. M. A., Stahel, E. P., Squire, D. R., and Stannett, V. T., Studies in Radiation-Induced Polymerization of Vinyl Monomers at High Dose Rates. II. Methyl Methacrylate. *J. Appl. Polym. Sci*. Vol 18, **1974**, pp.709-725.

[7] Schissel, S.M., Lapin, S.C., Jessop, J.L.P., Internal reference validation for EB-cured polymer conversions measured via Raman spectroscopy. *RadTech Rep*. 28(4), **2014**, pp. 46–50.

[8] Cai, Y., Jessop, J.L.P., Decreased oxygen inhibition in photopolymerized acrylate/epoxide hybrid polymer coatings as demonstrated by Raman spectroscopy. *Polym*. 47(19), **2006**, pp. 6560–6566.